PROCEEDINGS OF SCIENCE

Nucleon Electromagnetic and Axial Form Factors in a Light-front Constituent Quark Model

W. R. B. de Araújo*
Secretaria de Educação do Estado de São Paulo, DE Norte 2, Seduc SP, Brazil
E-mail: wilsonrbarbosa@prof.educacao.sp.gov.br

E. F.Suisso
Instituto Nacional de Propriedade Industrial,INPI, RJ, Brazil
E-mail: suisso@inpi.gov.br

J. P. B. C. de Melo
Laboratório de Física Teórica e Computacional - LFTC
Universidade Cruzeiro do Sul / Universidade Cidade de São Paulo, 01506-000 São Paulo, Brazil
E-mail: joao.mello@cruzeirodosul.edu.br

T. Frederico
Instituto Tecnológico de Aeronáutica, DCTA
12.228-900 São José dos Campos, SP, Brazil.
E-mail: tobias@ita.br

Kazuo Tsushima
Laboratório de Física Teórica e Computacional - LFTC
Universidade Cruzeiro do Sul / Universidade Cidade de São Paulo, 01506-000 São Paulo, Brazil
E-mail: kazuo.tsushima@cruzeirodosul.edu.br

In the present work we study the effect of the scalar spin coupling of constituent quarks on the nucleon electroweak properties by introducing a valence light-front wave function with two momentum scales. By comparing the results obtained with the one scale and two scale wave function models, we have found that the last one has shown a reasonable description of the static observables and $\mu_p G_{Ep}/G_{Mp}$ ratio in which the position of the zero appears around 10 [GeV/c]^2 or for higher squared momentum transfers. We have also shown results for the axial-vector coupling g_A and the nucleon axial-vector form factor. The best result for g_A was obtained when the parameters of the nucleon wave function model were such that the experimental value of the neutron magnetic moment was described.

XV International Workshop on Hadron Physics (XV Hadron Physics) 13 -17 September 2021
Online, hosted by Instituto Tecnológico de Aeronáutica, São José dos Campos, Brazil

*Speaker.

PoS(XVHadronPhysics)074

1. Effective Lagrangian for the N-q coupling

The first step in our model is to wrote down the effective Lagrangian

$$\mathscr{L}_{N-3q} = m_N \varepsilon^{lmn} \overline{\Psi}_{(l)} i\tau_2 \gamma_5 \Psi^C_{(m)} \overline{\Psi}_{(n)} \Psi_N + H.C., \tag{1.1}$$

which has been chosen to built a scalar spin coupling between a pair of quark fields $\overline{\Psi}_{(l)}$ and $\Psi^C_{(m)}$ with colorless nucleon field Ψ_N. One of the isospin matrices is τ_2; the color indices are l,m,n; the totally antisymmetric tensor in color space is ε^{lmn}. The charge conjugate field is $\Psi^C = C\overline{\Psi}^\top$, where $C = i\gamma^2\gamma^0$ is the charge conjugation matrix and m_N is the nucleon mass. Observe that through Fierz transform the spin structure of the nucleon becomes quite rich, despite the simple structure chosen for the effective Lagrangian.

2. Electromagnetic and Axial form factors

The matrix element of the plus component of the nucleon electromagnetic current ($J^+_N = J^0_N + J^3_N$), taking into account the Drell-Yan condition with $q^+ = q^0 + q^3 = 0$, is given by

$$\begin{aligned}\langle s'|J^+_N(Q^2)|s\rangle &= \bar{u}(p',s')\left(F_{1N}(Q^2)\gamma^+ + \imath\frac{\sigma^{+\mu}Q_\mu}{2m_N}F_{2N}(Q^2)\right)u(p,s)\\ &= \frac{p^+}{m_N}\langle s'|F_{1N}(Q^2) - \imath\frac{F_{2N}(Q^2)}{2m_N}\hat{n}\cdot(\vec{q}_\perp\times\vec{\sigma})|s\rangle\ ,\end{aligned}$$

where F_{1N} and F_{2N} are the Dirac and Pauli form factors, respectively, and $\hat{n}$ is the unit vector along the z-direction. The electric and magnetic Sachs form factors are written in terms of Pauli and Dirac and Pauli form factors, as:

$$G_{EN}(Q^2) = F_{1N}(Q^2) - \frac{Q^2}{4m_N^2}F_{2N}(Q^2) \quad \text{and} \quad G_{MN}(Q^2) = F_{1N}(Q^2) + F_{2N}(Q^2)\,. \tag{2.1}$$

From the above form factors we extract the charge radius as $r^2_N = -6\frac{dG_{EN}(Q^2)}{dQ^2}|_{Q^2=0}$ and the magnetic moment as $\mu_N = G_{MN}(Q^2=0)$.

From the plus component of the nucleon axial-vector current with the Drell-Yan condition we have that:

$$\langle s'|A^+_i(Q^2)|s\rangle = \bar{u}(p',s')G_A(Q^2)\gamma^+\gamma^5\frac{\tau_i}{2}u(p,s) = \frac{p^+}{m_N}G_A(Q^2)\langle s'|\frac{\tau_i}{2}\sigma_z|s\rangle\,, \tag{2.2}$$

with $g_A = G_A(0)$ being the axial-vector nucleon coupling. For both calculations of the electromagnetic and axial-vector form factors, we adopted the Breit frame. The squared momentum transfer is $Q^2 = -q^2 = q^2_\perp$, $p = (\sqrt{\frac{q^2_\perp}{4}+m^2_N}, -\frac{\vec{q}_\perp}{2}, 0)$ and $p' = (\sqrt{\frac{q^2_\perp}{4}+m^2_N}, \frac{\vec{q}_\perp}{2}, 0)$ are the nucleon momentum, before and after the absorption of the virtual photon, respectively.

The microscopic matrix elements of the electromagnetic and axial current are derived from the effective Lagrangian, Eq.(1.1), within the light-front impulse approximation which is represented by four three-dimensional diagrams in Fig.1 (left panel). The diagrams embody the antisymmetrization of the quark state in the wave function. In all diagrams from Fig.1 (left panel), the quark 3 is the quark which absorbs the momentum transfer carried by the virtual photon.

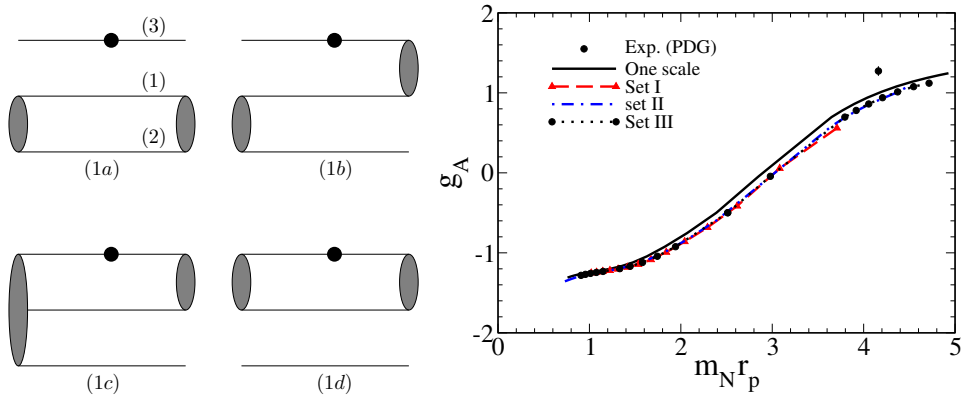

Figure 1: Left Panel: Diagrammatic representation of the nucleon photo-absorption amplitude. The gray blob represents the spin invariant for the coupled quark pair in the effective Lagrangian Eq. (1.1). The small filled circle attached to the quark line represents the action of the EM current operator. Right panel: Correlation between g_A and $m_N r_p$ calculated by the two-scale models (set I, set II, Set III) and one scale wave function. The experimental data from Ref. [5] is given by the filled circle.

The microscopic electromagnetic current for the nucleon depicted in the left panel of Fig.1 is given by

$$J_N^+(Q^2) = J_{aN}^+(Q^2) + 4J_{bN}^+(Q^2) + 2J_{cN}^+(Q^2) + 2J_{dN}^+(Q^2)\,, \tag{2.3}$$

and the axial-vector current is given by,

$$A_{AN}^+(Q^2) = A_{aN}^+(Q^2) + 4A_{bN}^+(Q^2) + 2A_{cN}^+(Q^2)\,. \tag{2.4}$$

For each of these microscopic currents, we performed the analytic integration over the quarks light-front energies k_i^- in the two-loop integral. After that, we have obtained two-loop three momentum integrations written in terms of the light front kinematical momenta. For instance, J_a^+ is given by

$$\begin{aligned} < s' \mid J_{aN}^+ \mid s >= 2p^+ m_N^2 < N \mid \hat{Q}_q \mid N > \int \frac{dk_1^+ d^2\vec{k}_{1\perp} dk_2^+ d^2\vec{k}_{2\perp}}{k_1^+ k_2^+ k_3^{+2}} \theta(p^+ - k_1^+)\theta(p^+ - k_1^+ - k_2^+) \\ \times Tr\left[(k_2 + m)(k_1 + m)\right] u(p',s')(\not{k}_3' + m)\gamma^+(\not{k}_3 + m)u(p,s)\Psi(M_0'^2)\Psi(M_0^2)\,, \end{aligned} \tag{2.5}$$

where M_0^2 and $M_0'^2$ are the squared free mass of the virtual three constituent quarks system in the initial and final nucleon, respectively.

In the same way, we have obtained J_{bN}^+, J_{cN}^+, J_{dN}^+. For the axial-vector current current, for instance A_{aN}^+, is given by

$$\begin{aligned} \langle s' | A_{aN}^+(Q^2) | s \rangle = 2p^{+2} m_N^2 \langle N | \frac{\vec{\tau}}{2} | N \rangle \int \frac{d^2k_{1\perp} dk_1^+ d^2k_{2\perp} dk_2^+}{k_1^+ k_2^+ k_3^{+\,2}} \theta(p^+ - k_1^+)\theta(p^+ - k_1^+ - k_2^+) \\ \times \mathrm{Tr}\left[(k_2 + m)(k_1 + m)\right] \bar{u}(p',s')(k_3' + m))\gamma^+\gamma^5(k_3 + m)u(p,s)\Psi(M_0'^2)\Psi(M_0^2)\,. \end{aligned} \tag{2.6}$$

Following the same steps for the nucleon axial-vector current $A_{aN}^+(Q^2)$, after integration over k_i^- we obtain $A_{bN}^+(Q^2)$, $A_{cN}^+(Q^2)$, and $A_{dN}^+(Q^2) = 0$ due to the isoscalar nature of the scalar quark pair.

3. Two scale wave function

The "two-scale model" of the momentum component of the valence light-front nucleon wave function [1, 2] was chosen to be represented by a power law form [3, 4] including two terms

$$\Psi_{\rm Power} = N_{\rm Power}\left[(1+M_0^2/\beta^2)^{-p} + \lambda(1+M_0^2/\beta_1^2)^{-p_1}\right] , \tag{3.1}$$

where

$$\lambda = (1+M_H^2/\beta_1^2)^{p_1}/(1+M_H^2/\beta^2)^{p} . \tag{3.2}$$

The characteristic momentum scales of the wave function (3.1) are represented by β, β_1 and M_H, where the low-momentum scale, $\beta \sim \Lambda_{QCD}$ is driven essentially by the nucleon static observables, while the high-momentum scales are driven by the zero of $G_{Ep}(Q^2)$ [1, 2]. The mass scale M_H gives the mass of the virtual three-quark system where the two terms in the wave function have the same magnitude. We associate this mass scale as a qualitative measure of the boundary separating the IR dynamics and the one-gluon exchange interaction dominance. Note that our choice corresponds to a node-less momentum component of the valence wave function in order to represent the nucleon ground state. The normalization constant $N_{\rm Power}$ is fixed to reproduce the proton charge.

Table 1: Parameters of one and two scales wave functions

Reference	β (GeV)	β_1 (GeV)	p	p_1	M_H (GeV)
Set I	1.07	10	3.4	3	3.68
Set II	0.396	10.56	3	3	5.92
Set III	0.34	7.5	3.2	3	4.32
One scale I	0.477	-	3	-	-
One scale II	1.07	-	3	-	-

4. Numerical Results

In our models we have used the constituent quark mass m of 220 MeV. In Table1, we show the parameters Set I and one scale II, chosen to reproduce the proton magnetic moment, μ_p, respectively, and Set II, Set III and one scale II, chosen to reproduce the neutron magnetic moment, μ_n, respectively. The static observables are preserved by introducing the second scale in the wave function. This can be checked by looking to Table 2.

The left panel in Fig.2 shows the $\mu_p G_{E_p}/G_{M_p}$ ratio as a function of the square momentum transfer for all the five models given in Table 1. The two scale models present the zero of the proton electric form factor for $Q_0^2 \sim 10$ GeV^2, showing a dramatic improvement over the one scale models in comparison to the experimental data. The introduction of the high momentum scale increases the probability of the three-quark system to be found with high virtuality, associated with the long tail of the momentum component of the wave function.

Our model shows a better description of the experimental data when the parameters are chosen to fit neutron magnetic moment. We have observed this behaviour for all nucleon electromagnetic

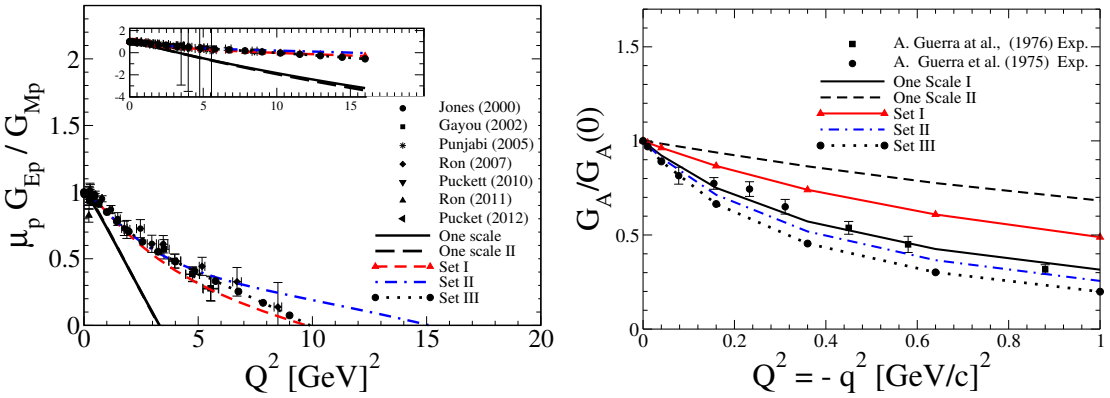

Figure 2: Left Panel: Proton electromagnetic form factor ratio $\mu_p G_{Ep}(Q^2)/G_{Mp}(Q^2)$, calculated by the two-scale (set I, set II, Set III) and one-scale I and II wave functions models. The experimental data are from Refs. [6, 7, 8, 9, 10, 11, 12, 13]. Right panel: Normalized axial-vector form factor, $G_A(Q^2)/G_A(0)$, calculated with the two-scale (set I, set II and set III), and one-scale (I and II) wave functions. Experimental data are from [14].

Table 2: Axial and Electromagnetic properties of nucleons, and the value of zero Q_0^2 of $G_{Ep}(Q_0^2) = 0$ obtained with the two-scale (set I and set II) and one-scale wave functions.

	g_A	μ_p (μ_N)	r_p (fm)	μ_n (μ_N)	r_n^2 (fm^2)	Q_0^2 (GeV^2)
Set I	0.56	2.80	0.78	-1.55	-0.07	8.27
Set II	0.97	3.05	0.94	-1.88	-0.06	15.12
Set III	1.09	3.11	1.00	-1.97	-1.01	9.94
One scale 1	1.01	3.11	1.03	-1.91	-0.08	3.28
One scale 2	0.52	2.79	0.75	-1.51	-0.10	3.28

and axial-vector form factors. For instance, the pattern shown in the right panel of Fig.2, was also found for the proton and neutron electromagnetic form factors.

5. Conclusion and Summary

We give a brief conclusion and summary from our work:

1. The two-scale nucleon wave function model carrying a high-momentum scale, can achieve a reasonable description of the ratio $\mu_p G_{Ep}(Q^2)/G_{Mp}(Q^2)$ and the position of its zero, without destroying the good outcomes provided by the one-scale wave function model in describing the nucleon static properties.

2. The best description of $\mu_p G_{Ep}/G_{Mp}$ and static observables is achieved by the introduction of the two-scale wave function with the parameters chosen to reproduce μ_n.

3. A good description of the nucleon electroweak observables, namely the axial-vector and electromagnetic form factors, is found when the wave function parameters are chosen to reproduce the neutron magnetic moment.

Acknowledgements: This work was supported in part by CAPES under Grant and by the Conselho Nacional de Desenvolvimento Científico e Tecnológico (CNPq), Grant No. 308486/2015-3 (TF), Process No. 307131/2020-3 (JPBCM), Grants No. 438562/2018-6 and Fundação de Amparo à Pesquisa do Estado de São Paulo (FAPESP), Process No. 2019/02923-5 (JPBCM), and was also part of the projects, Instituto Nacional de Ciência e Tecnologia – Nuclear Physics and Applications (INCT-FNA), Brazil, Process No. 464898/2014-5, and FAPESP Temático, Brazil, Process, the thematic projects, No. 2013/26258-4 and No. 2017/05660-0. KT was supported by the Conselho Nacional de Desenvolvimento Científico e Tecnológico (CNPq) Process, No. 313063/2018-4, and No. 426150/2018-0, and Fundação de amparo à Pesquisa do Estado de São Paulo (FAPESP) Process, No. 2019/00763-0.

References

[1] W. R. B. de Araújo, T. Frederico, M. Beyer and H. J. Weber, Eur. Phys. J. A 29 (2006) 227.

[2] W. R. B. de Araújo, J. P. B. C de Melo, K. Tsushima, Nucl.Phys. A970 (2018) 325-352.

[3] S. J. Brodsky and F. Schlumpf, Phys. Lett. B 329 (1994) 111; Prog. Part. Nucl. Phys. 34 (1995) 69.

[4] S. J. Brodsky, H.-C. Pauli and S. S. Pinsky, Phys. Rep. 301 (1998) 299.

[5] C. Patrignani et al. (Particle Data Group), Chin. Phys. C, 40 (2016) 100001.

[6] M. K. Jones et al.[Jefferson Lab Hall A collaboration], Phys. Rev. Lett. 84 (2000) 1398.

[7] E. J. Brash, A. Koslov, Sh. Li and G. M. Huber, Phys. Rev. C 65 (R) (2002) 051001.

[8] O. Gayou et al., Phys. Rev. Lett. 88 (2002) 092301.

[9] V. Punjabi *et al.*, Phys. Rev. C 71 (2005) 055202; Erratum: [Phys. Rev. C 71 (2005) 069902].

[10] G. Ron *et al.*, Phys. Rev. Lett. 99 (2007) 202002.

[11] A. J. R. Puckett *et al.*, Phys. Rev. Lett. 104 (2010) 242301.

[12] G. Ron *et al.* [Jefferson Lab Hall A Collaboration], Phys. Rev. C 84 (2011) 055204.

[13] A. J. R. Puckett *et al.*, GeV^2," Phys. Rev. C 85 (2012) 045203.

[14] A.Del. Guerra et al., Nucl.Phys.B 99(1975) 253; ibid., Nucl.Phys.B107(1976) 65.